

Research paper

An experimental analysis of quenching of continuously heated vertical rod with aqueous Al₂O₃ nanofluid



Nirupama Patra^{a,*}, Vivek Gupta^b, Ravi Singh^b, R.S. Singh^a, Pradyumna Ghosh^b, Arun Nayak^c

^a Department of Chemical Engineering, IIT (BHU), Varanasi 221005, UP, India

^b Department of Mechanical Engineering, IIT (BHU), Varanasi 221005, UP, India

^c Reactor Engineering Division, BARC, Mumbai, India

ARTICLE INFO

Article history:

Received 19 June 2016

Accepted 22 February 2017

Available online 18 April 2017

Keywords:

Decay heat

Nanofluid

Quenching

ABSTRACT

Quenching characteristics of metallic vertical rod with an internal heater has been investigated in pure water and water-based nanofluid with alumina nanoparticles of 0.001% by volume. Initial temperature of the testing rod (12 mm diameter and 1000 mm length) ranges from 200 °C to 250 °C. The internal heater may be used to simulate the decay heat generated by the nuclear fuel rod after the power plant shut-down. Tests have been performed with varied range of experimental conditions of decay heat, constant water and nanofluid flow rates. The cooling curves follow a general trend of a rapid temperature drop up to almost 100 °C of the rod surface temperature irrespective of the operating parameters and the location of the thermocouple. The obtained results during quenching process indicated that HTC (heat transfer coefficient) for nanofluids are more than de-ionized water. It was also observed that in identical circumstances, the quenching time of the specimen in Al₂O₃ nanofluid considerably decreased as compared to water. The results exhibit that nanofluids can enhance the reflood heat transfer performance in terms of quenching rate for a long vertical rod causing liquid-droplets-induced depositions of nanoparticles resulting in making a pre-coating effect characterized by higher wettability.

© 2017 Tomsk Polytechnic University. Published by Elsevier B.V.

This is an open access article under the CC BY-NC-ND license.

(<http://creativecommons.org/licenses/by-nc-nd/4.0/>)

1. Introduction

Quenching (rewetting) is an important phenomenon for analysis of the heat removal from the fuel rod during a loss of coolant accident (LOCA) in a nuclear reactor and the reflood happens when water refills the reactor vessel and cools down the fuel rod at the time of the severe accident in nuclear power plant [1]. With the rapid development of nuclear energy worldwide, nuclear power plants produce a large amount of radioactive wastewater which can be treated by applying techniques such as filtration, chemical precipitation, biological methods, membrane processes and so on [2–5]. The quenching process is the rapid cooling of high temperature objects by exposure to a much cooler liquid, and is frequently used in several engineering applications, such as metallurgy and nuclear industries. The behavior of quenching process is generally influenced by many parameters, such as the surface

properties of the substance, thermal–hydraulic properties of the coolant, and temperatures of the substance and coolant [6]. In this process the heat transfer from a solid wall to adjacent liquid is limited by the occurrence of film boiling in which a stable vapor film layer covers the hot solid surface. Thus an acceleration of the transition from film boiling to nucleate boiling is often desirable, as it results in a much higher heat transfer rate. Because the conventional fluids are not capable of achieving the desired heat transfer rate, the nanofluids are expected to accelerate this transition.

In recent years, the effects of nanofluids on the quenching behaviors have been studied extensively in the literature. Kim et al. [7] studied the quenching behavior of steel and zircaloy spheres in pure water and water-based alumina, silica, and diamond nanofluids. The initial temperatures of the testing spheres were controlled to be as high as 1030 °C. They stated that the surface roughness increase and wettability enhancement may be responsible for the early disruption of the film boiling and the enhancement of quenching due to nanoparticle deposition. The effect of deposited nanoparticles on the quenching behavior of a metallic rod

* Corresponding author. Department of Chemical Engineering and Technology, IIT (BHU), Varanasi 221005, India. Tel.: +91 8765449287.

E-mail address: npatra.rs.che13@itbhu.ac.in (N. Patra).

in water-based nanofluids was further established by Kim et al. [8], and Ciloglu and Bolukbasi [9]. Chun et al. [10] conducted quenching experiments of the bare Pt wires and Si/SiC nanoparticle-coated Pt wires in water and nanofluids containing Si and SiC, respectively. The authors found that for the bare Pt wires there was no significant influence on boiling curve between water, Si and SiC nanofluids. However, the authors observed a rapid cooling without stable film boiling for nanoparticle-coated Pt wires. They pointed that this phenomenon depended on the macrostructure and the thickness of nanoparticle deposition layer.

Prakash Narayan et al. [11] analyzed the effect of boiling surface roughness on heat transfer rate in Al_2O_3 nanofluid with particles of different diameters. They found that higher values of boiling surface roughness enhanced heat transfer rates. Also, they observed that the ratio of average particle size to average roughness of the boiling surface was effective in rate of heat transfer in nanofluid pool boiling. Lotfi and Shafii [12] conducted experiments on a high temperature silver sphere in Ag, TiO_2 /water nanofluids to investigate quenching characteristics of nanofluids. The authors shown that the quenching process was more rapid in pure water than in nanofluids and the cooling time decreased with increase in nanoparticle concentration. They found that nanoparticle deposition on the sphere surface acted as a thermal insulator for the sphere due to the higher thermal resistance of the TiO_2 layer. Prasanna Kumar [13] conducted experiments to study the heat transfer behaviors during the quenching of two different types of steel rod (low alloy steel and plain carbon steel) with an initial rod temperature of about $850^\circ C$ in a mineral oil and polymer solution. They concluded that the maximum quenching rates for the both steel rods occurred between $600^\circ C$ and $700^\circ C$, which were also reported by Hasan et al. [14] for steel rods with a variety of iron alloys at the same initial temperature using mineral oil and polymer solution. In addition, Prasanna Kumar [13] found that the surface heat flux in the mineral oil was slightly smaller than that in the polymer solution. Lee et al. [15] studied the quenching behavior of a long SS tube (1.6 m) with an initial temperature of $600\text{--}700^\circ C$ in a 3.5% sea salt solution (close to the concentration of natural sea water). They found that the quenching time of the tube in the sea salt solution was shortened by 10 s (8.4%) and the CHF was enhanced by 9.7% as compared to water, caused by the earlier condensation of vapor during the reflood of the sea salt solution. Hsu et al. [16] conducted experiments on the quenching of stainless steel and zircaloy spheres at the initial temperature of about $1000^\circ C$ in both natural sea and deionized water with the pool temperature of $33^\circ C$. The quenching curves (i.e., temperature vs. time) and visualization results of their study demonstrated that the film boiling was clearly observed in deionized water but not in sea water. The formation of vapor film in water was through the coalescence of bubbles nucleated at a very high temperature. More rapid quenching was revealed in sea water due to the quenching process starting with transition boiling and the absence of film boiling.

Babu and Prasanna Kumar [17] determined the surface heat flux and temperature using the Inverse Heat Conduction method during quenching and modeled the surface heat flux as a function of dimensionless parameters. Choi [18] has demonstrated the possibility of using nanofluids for various practical applications which include quenching. Babu and Prasanna Kumar [19] demonstrated the use of nanofluids as coolants to improve the quenching heat transfer by quenching stainless steel probes in CNT nanofluids and found that nanofluids improve the quenching heat transfer rate as compared to water. In another work [20] they have studied the effect of CNT nanofluid on the quenching heat transfer based on the estimated heat flux and surface temperature at the quenched surface. They have shown that nanofluids improved quenching heat transfer rate significantly as compared with that of water. Paul et al.

[21] studied the effect of different parameters such as the rate of coolant injection, initial pipe wall temperature ($300\text{--}500^\circ C$), and concentration of dispersed nanoparticles (0.1 vol % and 0.3 vol % Al_2O_3 -water nanofluids) on the quenching behavior. The authors have shown that the nanofluid takes lesser time to cool as compared to water and the rate of cooling increases with the increase in concentration of Al_2O_3 particles in the nanofluid.

So far, quenching experiments have been performed mostly with rods, tubes and spheres with a wide range of experimental conditions with several types of working fluids. The heat transfer mechanism during top flooding of a hot cylindrical rod similar to a nuclear pin by a continuous falling film has not been focused extensively in the literature. The objective of the present study was to investigate and compare the quenching of a typical nuclear fuel rod with a long length of about 980 mm using deionized (DI) water and alumina nanofluid (NF) as a function of decay heat (DH). The testing rod, made of Stainless Steel (SS316L) was continuously heated during the quenching process to simulate the decay heat generated by the nuclear fuel rod after the power plant shutdown. The effect of several parameters like coolant flow rate, initial dry wall temperature and decay heat on the quenching process are investigated to obtain a suitable comparison of the performance between nanofluids and water for non continuously heated (NCH) and continuously heated condition of the heater.

2. Materials and methods

2.1. Preparation and characterization of nanofluid

Preparation of nanofluid is an important step for changing heat transfer performance of conventional base fluids. Nanofluid refers to a new class of heat transfer fluids prepared by dispersing nanoparticles into conventional fluids and should have stable suspension, minimal agglomeration of particles and no chemical change of the fluid. So, the following methods are used for preparation of effective suspensions such as changing the pH value, using surface activators and/or dispersants, and using ultrasonic vibrations [22].

Concentrated water based dispersion of alumina nanoparticles was acquired from Alfa Aesar, A Johnson Matthey Company. The vendor-specified concentration was 23% by weight for alumina. In the present study an Ultrasonic Bath (MJL Laboratory Instruments & Equipments, 500 W, ultrasonic frequency 30 ± 3 KHz) was used to prepare Al_2O_3 -water nanofluid. The purchased alumina dispersion was diluted with DI water to the concentration of interest for the quenching experiments, i.e., 0.001 vol.% by subjecting to 2 hour of sonication in the ultrasonic bath. No surfactant or buffer was added to the nanofluids during dilution.

The simplest and most widely used method is XRD (X-Ray Diffraction) for estimating the average nanoparticle grain size. The purchased Al_2O_3 nanofluid was diluted with distilled water followed by centrifugation at 3000 rpm for 90 min. Then the settled nanoparticles were washed with absolute ethanol and acetone. Further these were vacuum dried at $80^\circ C$ for 2 hour in the oven. The obtained Al_2O_3 nanopowder was characterized by XRD with a Rigaku X-ray Diffractometer and Cu-k $\alpha 1$ radiation in the range of $20\text{--}80^\circ$. The X-ray diffraction test was carried out with a scan speed of $3^\circ/\text{minute}$. The average grain size was estimated by using Debye-Scherrer formula. The full width at half maximum (FWHM) was taken from the XRD pattern shown in Fig. 1.

$$d = \frac{0.9\lambda}{(FWHM)\cos\theta}$$

where 'd', ' λ ', and ' θ ' are the average particle grain size, wavelength of the Cu-k $\alpha 1$ X rays (1.5418\AA) and Bragg's angle respectively.

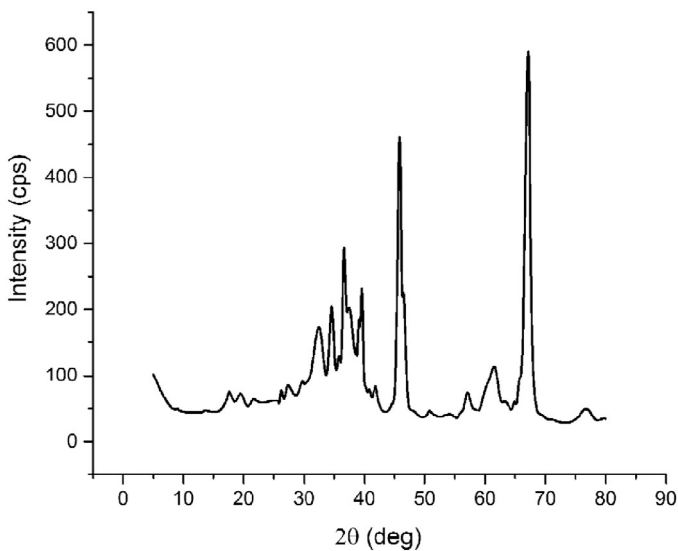


Fig. 1. XRD pattern of alumina nanoparticle.

The average grain size of alumina nanoparticle was found to be between 20 and 25 nm by using the Scherrer formula.

The thermo physical properties were measured for the suspensions of 0.001% Al_2O_3 nanofluid. The thermal conductivity of the suspensions were measured using a Hot Disk TPS500 device based on the transient plane source method. The rheological behaviors of the suspensions were measured using a Brookfield DVI rotational viscometer with a temperature-controlled bath. Before any set of measurement, the viscometer and the thermal analyzer were calibrated by using Brookfield viscosity standard fluids and DI water, respectively. Each measurement was repeated at least ten times to calculate the mean value of the experimental data. The uncertainty of these measurements was estimated to be within $\pm 1.5\%$.

The nanofluid density was calculated as $\rho_p\varphi + \rho_f(1 - \varphi)$, where φ is the nanoparticle volumetric fraction, and ρ_p and ρ_f are the density of the nanoparticle material and base fluid, respectively. The nanofluid heat capacity was determined as $[\rho_p C_p \varphi + \rho_f C_f (1 - \varphi)] / [\rho_p \varphi + \rho_f (1 - \varphi)]$, where C_p and C_f are the specific heat of the nanoparticle material and base fluid, respectively [23]. All the nanofluid properties were found to be within $\pm 4.5\%$ of those of pure water because of low concentration of nanoparticles used in this work. As such, thermo-physical properties effects are not expected to be significant in our quenching experiments. The thermal conductivity and viscosity values of water and Alumina nanofluid are listed in Table 1.

2.2. Experimental setup

The experimental facility was designed in such a manner that thermal-hydraulic phenomena associated with quenching of heater rod can be investigated. The main components of the experimental setup used in the present study were shown in Fig. 2. The setup

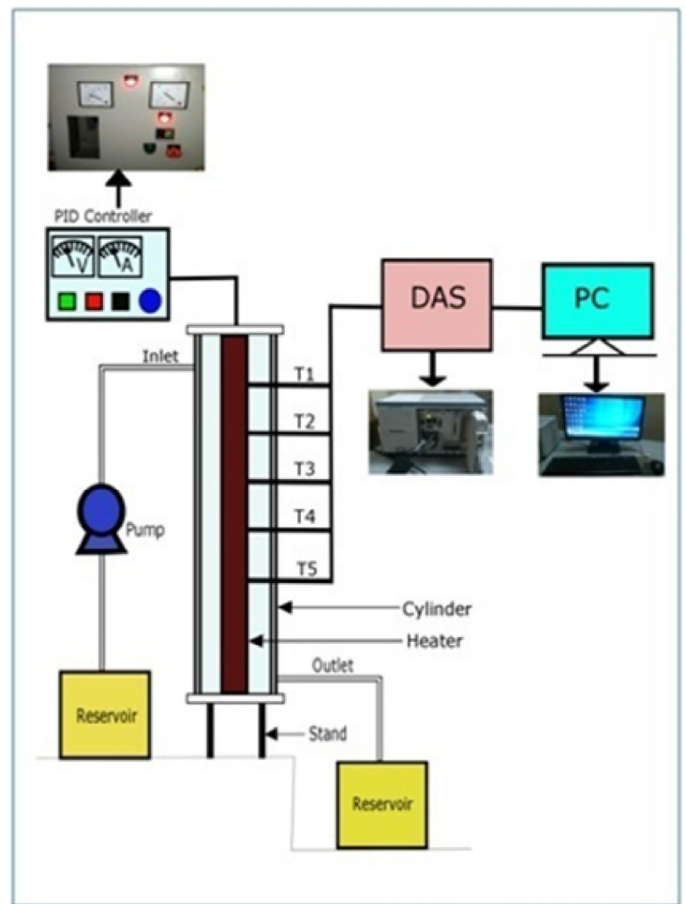


Fig. 2. Quenching experimental setup.

essentially consists of test section assembly, circulating pump, storage reservoir, PID controller, Data Acquisition System (DAS) and a personal computer. The experimental facility allows for varying the heat flux, flow rate, decay heat and initial temperature of the heater rod.

The test section assembly consists of a quartz cylindrical tube concentrically surrounding a cartridge heater (manufactured by Marathon Heater Pvt. Ltd, India). The cartridge heater of 12 mm outer diameter stainless steel (SS316 L) tube is heated by a uniformly heated electric coil with an inbuilt K-type thermocouple to control the heater temperature. The heater surface has a length of 980 mm with unheated portion of 100 mm and 50 mm at the bottom and top respectively. The heater can sustain a maximum power input of 10 kW. Power is supplied to the heater through the PID controller which can be operated either in manual mode or in auto mode. In the present work, manual mode is chosen so that power supply can be controlled easily and effectively. Provisions are made for the thermal expansion and contraction during heating and rapid cooling of the heater. The lower end of the heater tube is guided through a Teflon gasket (which can withstand high temperature) at the centre of the quartz cylinder which is fixed to the lower stainless steel flange. This is expected to minimize any buckling of the heater tube due to uneven thermal expansion during the experiment.

The quartz cylinder is 1000 mm long and 45 mm inner dia. and has an inlet opening at a distance of 20 mm from top and an outlet at 30 mm from the bottom. Two K-type thermocouples were inserted into the flow to measure the fluid bulk temperatures at the

Table 1

Measured thermal conductivity and viscosity values of water and Alumina nanofluid at 35 °C (Uncertainty 4.5%).

Material	Volume concentration	Dynamic viscosity (cP)	Thermal conductivity (W/mK)
DI water	–	0.70	0.633
Al_2O_3	0.001%	0.73	0.662

inlet and exit of the test section, respectively. The K-type thermocouple was used as it provides more accurate reading for high temperature measurements. The outer diameter of the K-type thermocouple used is 3 mm and its time constant provided by the manufacturer (OMEGA Inc.) is about 0.60 s in water. The quartz tube was drilled at five points and at each point two thermocouples were inserted, one was attached to heater surface for measuring surface temperature, T_s and other was left open in the fluid for measuring the fluid temperature, T_f . Five surface-type thermocouples were brazed to the heater surface at a distance of 0.08m, 0.28m, 0.48m, 0.68m, 0.88m from the top of the test section respectively. These thermocouples serve to monitor the wall temperature along the heater rod. The thermocouple wires at these locations were designated as T_{s1} through T_{s5} . The fluid temperature thermocouples are inserted just above the surface temperature thermocouples and measure the temperature of the fluid very close to the surface of the cylinder. All the thermocouples were connected to data acquisition system (National Instruments PXIe 1071). The thermocouples were used to measure the temperature during the quenching experiments and data acquisition system was to record the signals from the thermocouples using Lab view software. In addition, the personal computer was used to connect and record all the temperature data.

3. Experimental procedure

The present experimental study on quenching was carried out at atmospheric condition. The experiment was initiated by supplying electric power to the heater under dry condition. During heating, the surface temperature and the electric power level are monitored through the DAS and PID Controller, respectively. The supply of electric power to the heater is manually controlled to obtain the required wall temperature. After reaching the steady state condition, the power level is maintained at a constant value. After adjusting the flow rate, to initiate the quenching, the power supply to the heater rod is turned off for non-continuously heated (NCH) condition and a low value of heat flux is supplied throughout the quenching process to study the effect of decay heat (DH). At this stage, the circulation pump is turned on and the working fluid is directed to flow through inlet to the heater tube. The fluid from the outlet of the test section is drained and the reservoir is refilled after each experimental run when water is used as the working fluid. However, during experimentation with nanofluids, to minimize the cost and effort involved with the preparation, the temperature of the nanofluid stored in the reservoir is monitored continuously till ambient temperature is reached. The same procedure is followed for various initial wall temperatures and coolant flow rates. Pure water and nanofluids are used as the cooling liquid at saturated and highly subcooled ($\Delta T_{sub} = 70^\circ\text{C}$) state, always at atmospheric pressure.

It is obvious that the phenomenon of quenching depends on the mode of interaction of working fluid with the hot surface [24]. To approach the more real condition of the quenching of nuclear fuel pins in a nuclear power plant, the focus of the present study is to investigate the quenching of a vertical rod similar to single nuclear pin in DI water and 0.001% alumina nanofluid. The testing rod was continuously heated during the quenching process to study the effect of decay heat generated by the nuclear fuel rod after the power plant shutdown. In literature, no study on the quenching of a continuously-heated vertical rod using nanofluid was reported. In this study, the quenching curve, effect of flow rate and effect of initial temperature of the rod on quenching rate were investigated with or without continuously heating of the testing rod.

The rate of heat transfer (q) of the test specimen under transient conditions is assumed to be proportional to the temperature

Table 2

Thermo-physical properties of the test specimen [24].

Material of test specimen	SS316L
Density (ρ), kg/m ³	8000
Specific heat capacity (C), kJ/kg°C	0.420
Thermal conductivity (k), W/m°C	20

Table 3

Test matrix of experiment.

Test section characteristics	
Geometry	
Outer diameter	50 mm
Inner diameter	45 mm
Heater characteristics	
Geometry	
Diameter	stainless steel 316L cylindrical rod
Length	12 mm
Surface condition	980 mm
Power rating	Bare
Pressure	10 kW
Operating parameters	1.01325 bar
Working fluid	DI water and 0.001% Al ₂ O ₃ NF
Flow rate	7, 9 (g/s)
Initial rod temperature	200, 250 (°C)
Decay heat	0 (NCH), 7.992, 14.557 (kW/m ²)

gradient and can be expressed as:

$$q = -\rho C \left(\frac{V}{A} \right) \frac{dT}{dt} \quad (1)$$

Where ρ and C are the heater rod (SS316L) density and specific heat, respectively. V and A are the test specimen volume and surface area, respectively, dT/dt is the change in temperature (T) of a given location with respect to time (t). In this work, maximum initial test surface temperature is maintained at 250°C . For this temperature, variation in material properties such as: density and specific heat are found to be negligible. Therefore, constant value of C and ρ are considered in the analysis. The thermo-physical properties of the test specimen (SS316L) are listed in Table 2. The range of operating parameters used in the present experimental study is listed in Table 3. The temperature transient was recorded through data acquisition system and used to determine heat flux distribution.

The surface heat transfer coefficient can be calculated by:

$$h = \frac{q}{\Delta T} \quad (2)$$

Where ΔT is the difference between wall temperature and falling liquid film temperature at a given location.

The uncertainty analyses were performed using the method proposed by Holman [25]. Temperature measurement uncertainties were primarily estimated considering the thermocouple calibration and temperature correction from the thermocouple reading to the reference surface. The maximum variation of the measured wall temperatures of the heater rod and bulk fluid temperatures (k-type thermocouples) was $\pm 0.5^\circ\text{C}$. The present experimental study involves the measurement of various parameters, such as coolant flow rate, initial temperature of test specimen, and length and diameter of the test specimen. Considering errors in all the measuring parameters, the maximum uncertainty during calculation of heat transfer coefficient and surface heat flux is found to be less than .6.9% and 7.7% respectively.

4. Results and discussions

All quenching experiments were conducted with fixed inlet sub-cooling under atmospheric pressure condition. The experimental runs were carried out with non-continuously heated and continuously heated (as variation in DH) rod using DI water and 0.001

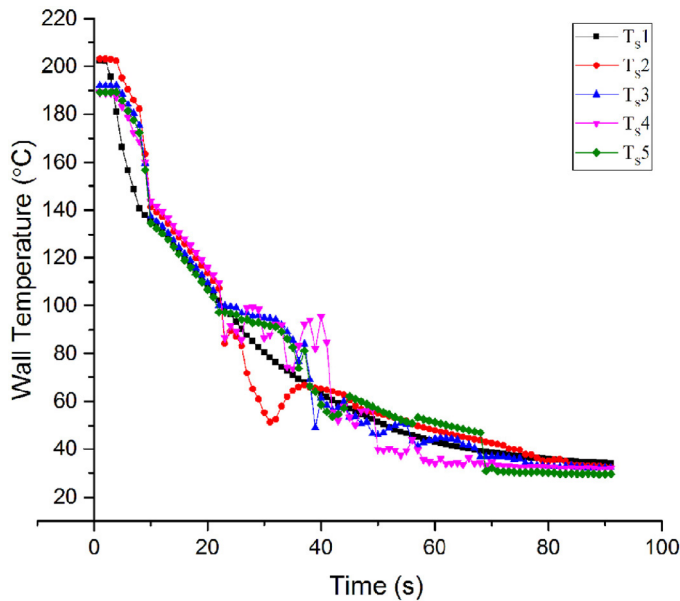


Fig. 3. Temperature–time traces from different thermocouples ($T_{s,1}$, $T_{s,2}$, $T_{s,3}$, $T_{s,4}$, $T_{s,5}$ at a distance of 0.08, 0.28, 0.48, 0.68, 0.88 (m) from the top respectively) quenched from 200 °C, coolant flow rate of 9 g/s (DI water for NCH condition).

vol. % Al_2O_3 –water nanofluid. The subcooled working fluid at room temperature enters through the inlet at the top of the vertical test section and exits through the outlet at the bottom. To ensure the repeatability during quenching reference data were obtained. The results of these repeatability tests, which we refer to as repeatable quenching has been analyzed and the quenching curve is reasonably repeatable with some minor data scattering.

When a hot vertical surface is quenched by the falling film of the liquid coolant, the typical temperature–time curve could be as shown in Fig. 3. The curve reveals that different mechanisms of heat transfer become prominent which are shown by the abrupt changes in the slope of the curve. As the initial rod temperature was not very high from the saturation temperature of the coolant, it may be assumed that initially quenching will be mainly through nucleate boiling and transition boiling. The occurrence of film boiling at this temperature is rather remote. The instantaneous drastic reduction in temperature during the first few seconds demonstrates this fact. After the fast decrease, the rate of cooling decreases. It may be noted that the first phase of intense cooling extends up to a rod temperature of 90–100 °C. However, fluctuations appear in the quenching curves as the temperature falls below 100 °C. This may be caused by the upward flow of generated steam in the test section. This phenomenon aggravates when decay heat is applied as the heater rod is continuously heated. The graph indicates that temporary breakup of the liquid film by the faster moving vapor streams might have caused the fluctuations. So while studying the effect of flow rate, initial rod temperature and decay heat, the graphs are plotted up to 100 °C.

4.1. Effect of initial rod temperature

A higher initial wall temperature implies that more heat needs to be removed from the wall before quenching can take place as shown in Fig. 4. The magnitude of heat transfer to the flowing coolant depends upon the initial surface temperature of the specimen, the temperature gradient and the local hydrodynamics [26].

The wall temperature behavior for the nanofluid was compared with those for the water during quenching at a fixed flow rate (7 g/s) for both NCH case and continuously heated case with two

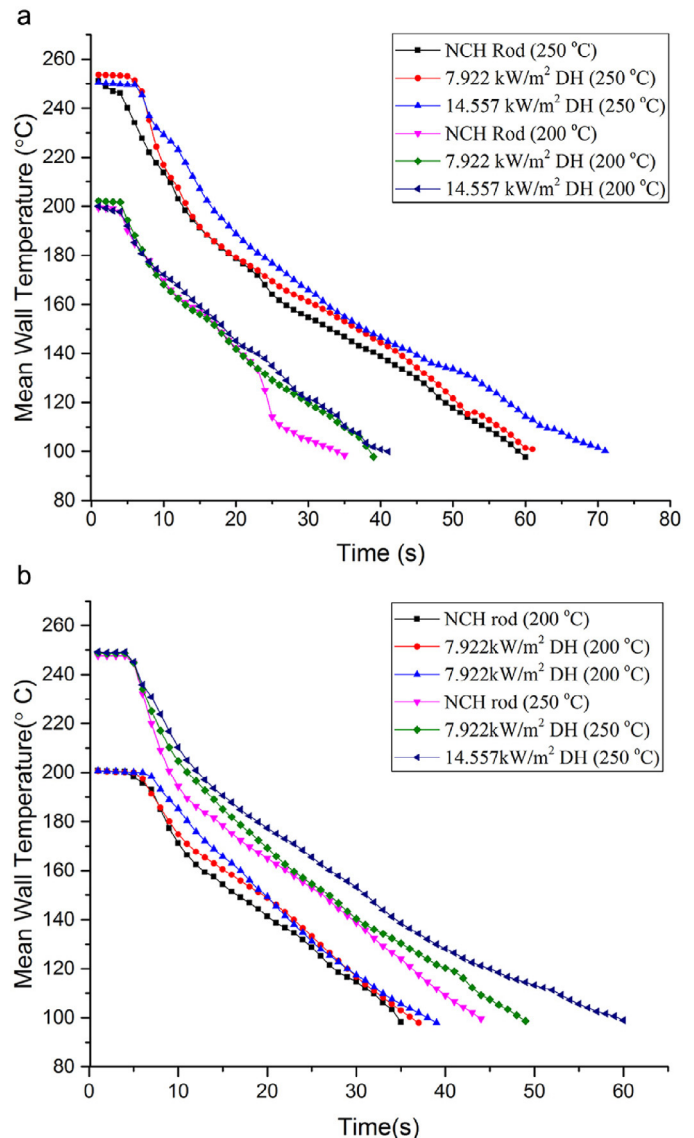


Fig. 4. Quenching Curves for the effect of Initial Wall Temperature with coolant flow rate of 7 g/s.

(a) DI water
(b) Alumina Nanofluid

values of decay heat. In the comparison between the water and the Al_2O_3 –water nanofluid, a difference in the quenching time (the time required to cool down the hot rod surface from the coolant injection to the termination of a quenching phenomenon, $T_{\text{wall}} = 100$ °C) is observed. From the graph (Fig. 4), it is evident that the effect of decay heat is not significant at lower value of initial rod temperature (200 °C). In addition, there is no considerable difference in quenching time between water and alumina NF for NCH case and continuously heated case when quenched from 200 °C. However, at higher initial temperature (250 °C), quenching time increases with increase in decay heat as because rods with a higher initial temperature will possess a large amount of stored heat and the applied decay heat will add to it. The difference in the quenching time between the water and the alumina NF shows more than 10 s for the decay heat of 14.557 kW/m². Indeed, the results exhibit that the continuous heat generation in the testing rod increases the cooling time of the quenching in deionized water as well as nanofluid, but the quenching rate (slope of the quenching curve) in nanofluid is more as compared to DI water.

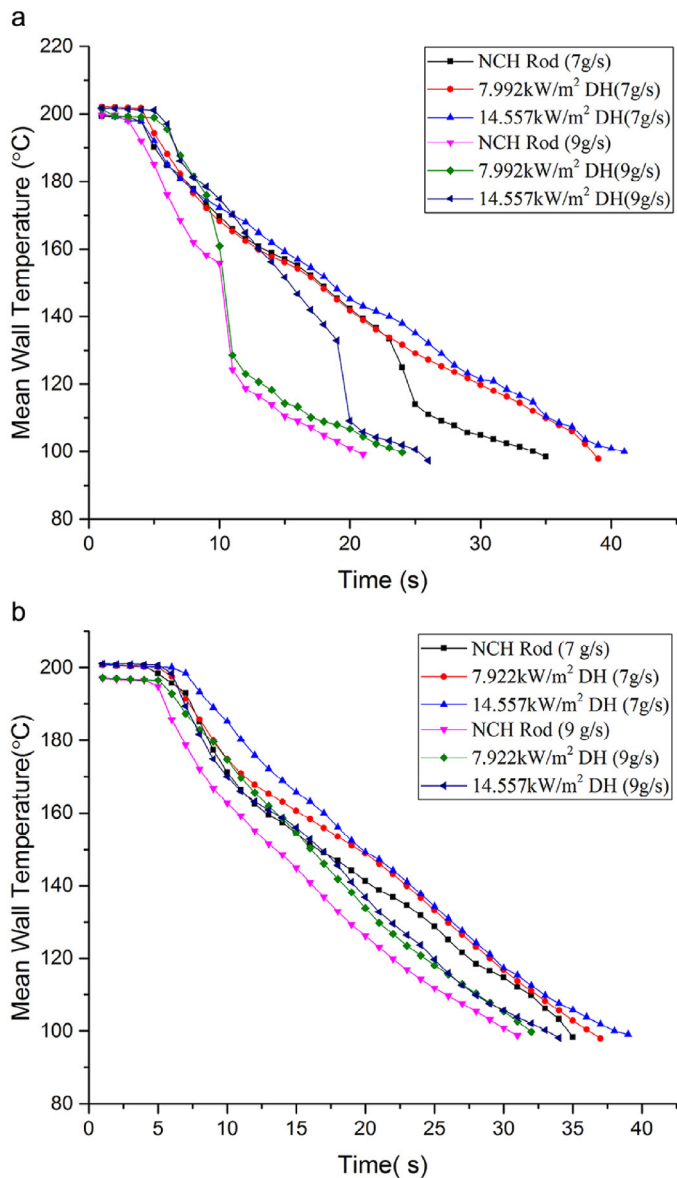


Fig. 5. Quenching Curves for the effect of flow rate at initial rod temperature of 200 °C.

(a) DI water
(b) Alumina Nanofluid

The enhanced cooling performance is attributed to high wettability of heating surface by deposition of nanoparticles during evaporation. During the quenching process, the liquid droplets carrying nanoparticles, which are dispersed into vapor, can be deposited on heating surface before fluids are moved forward. This phenomenon is more prominent in case of long tubes having small diameter. So, the thin layer of nanoparticles can be formed in advance resulting in making a pre-coating effect characterized by higher wettability [27].

4.2. Effect of flow rate

The increase in coolant flow rate results in the increase of the quenching rate for both water and nanofluid which contributes to the decrease in quenching time as shown in Fig. 5. An increase in the coolant flow rate causes a substantial extension of the nucleate boiling region and the quenching curve shifts towards left in case of DI water which can be observed in Fig. 5a. It is clear

that the quenching time for NCH rod for both the flow rates is less than continuously heated rod with decay heat. But no considerable change in quenching time is observed when the rod is quenched from a fixed temperature of 200 °C with decay heat of 7.992 and 14.557 kW/m² respectively for both the flow rates in case of DI water.

However, the effect of flow rate and decay heat is not significant on quenching time when the rod is quenched from an initial temperature of 200 °C using alumina nanofluid as shown in Fig. 5b. The reason may be attributed to the lower value of initial rod temperature because of which the evaporation of nanofluid droplets is hindered due to lower amount of heat stored in the rod. The lower stored heat, even when the decay heat is added to it, is not capable of evaporating the nanofluid leading to negligible change in quenching rate.

4.3. Effect of decay heat on heat transfer coefficient

The quenching heat transfer coefficient using deionized water and water based alumina nanofluid have been compared along the length of the heater rod measured from the top as shown in Fig. 6. The quench front which begins at the top of the heater rod (at the inlet) travels along the length and covers the entire length almost in 20–25 seconds. Hence, heat transfer coefficient has been evaluated considering the temperature-time data after 30 seconds from the commencement of quenching. The distance is measured from top of the test section which has been shown in graph (Fig. 6a and b). Heat transfer coefficients have been calculated at the thermocouple locations using the temperature data from the data acquisition system. It is observed that heat transfer coefficient for both water and nanofluids decreases in the downstream direction away from inlet where quenching begins. When the fluid jet impinges on the hot surface, the value of the heat transfer coefficient is maximum at this point. However, the surface temperature of the heated rod decreases in the downstream direction. It is observed that the locations, away from inlet come in contact with the liquid with lower liquid sub-cooling and increased enthalpy. A fluid with higher enthalpy has less capacity to extract heat from the hot surface. Therefore surface heat flux reduces at the location away from the inlet.

However, the heat transfer coefficient is enhanced considerably in nanofluids as compared to DI water due to depositions of nanoparticles during evaporation of liquid droplets for both NCH case as well as continuously heated with decay heat of 14.557 kW/m². The effect of decay heat is not significant because the heat transfer coefficient mainly depends on stored heat which is dependent on initial rod temperature.

The heat transfer enhancement phenomenon can be illustrated as the formation of nanoparticle embedded surface due to scattered deposition of nanoparticles. As a result, it increases the effective surface area of heat transfer as well as the turbulence near the surface. However, the combined effect of increasing heat transfer surface area, turbulence and thermo physical properties of fluid leads to the increment in heat transfer as well as heat transfer coefficient in nanofluids as compared to water.

5. Conclusions

The present experiments were conducted to investigate the effect of nanofluids on quenching heat transfer of a hot vertical rod with different operating parameters. The testing rod made of Stainless Steel (SS316L), coupled with an internal heater, was continuously heated during the quenching process to explore the effect of decay heat generated by a nuclear fuel rod after the reactor shutdown.

The following results are obtained.

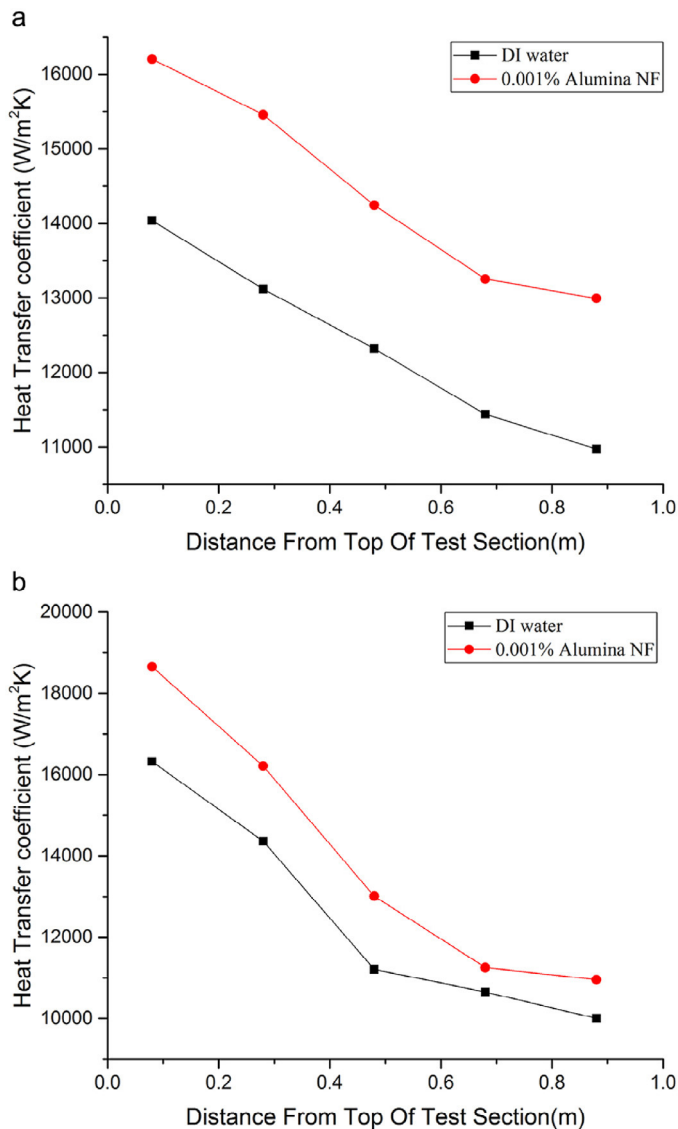


Fig. 6. Variation of heat transfer coefficient with axial location for initial rod temperature 250 °C, flow rate 7 g/s.

(a) Non-Continuously heated Case

(b) Continuously heated Case with DH of 14.557 KW/m²

- (1) The quenching tests have been performed using nanofluids as well as DI water. A more enhanced cooling performance is observed in the case of nanofluid quenching.
- (2) The enhanced cooling performance is due to high wettability of a thin layer formed on a heating surface by a deposition of nanoparticles during evaporation of liquid droplets. This phenomenon is more prominent in case of a long rod.
- (3) The quenching performance is enhanced more than 10 s for Al₂O₃-water nanofluid in comparison to DI water at higher initial rod temperature. The effect of decay heat is more significant at higher initial rod temperature.
- (4) The effect of flow rate on quenching time is not significant for both water and nanofluid; however, the study can be conducted at higher value of initial rod temperature and wide range of flow rate to conclude in a better way.
- (5) The heat transfer coefficient is enhanced in case of nanofluids as compared to DI water in both the cases, with or without decay heat. The effect of decay heat is not significant because the

heat transfer coefficient mainly depends on stored heat which is dependent on initial rod temperature.

Acknowledgement

The financial support provided by Board of Research in Nuclear Sciences (BRNS, DAE, INDIA) (2013/36/73-BRNS/10617) is gratefully acknowledged.

References

- [1] S.W. Lee, S.Y. Chun, C.H. Song, I.C. Bang, Effect of nanofluids on reflow heat transfer in a long vertical tube, *Int. J. Heat Mass Transf* 55 (2012) 4766–4771.
- [2] M. Ganesapillai, P. Simha, The rationale for alternative fertilization: equilibrium isotherm, kinetics and mass transfer analysis for urea-nitrogen adsorption from cow urine, *Resour. Effic. Technol* 1 (2015) 90–97.
- [3] P. Simha, M. Mathew, P. Jain, M. Ganesapillai, Resource recovery and recycling in sanitation is key to health, water and food security, 2015.
- [4] M. Ganesapillai, A. Singh, P. Simha, Separation processes and technologies as the mainstay in chemical, biochemical, petroleum and environmental engineering: a special issue, *Resour. Effic. Technol* 2 (Suppl. 1) (2016) S1–S2.
- [5] P. Simha, A. Yadav, D. Pinjari, A.B. Pandit, On the behaviour, mechanistic modelling and interaction of biochar and crop fertilizers in aqueous solutions, *Resour. Effic. Technol* 2 (2016) 133–142.
- [6] B.-R. Fu, Y.-H. Ho, M.-X. Ho, C. Pan, Quenching characteristics of a continuously-heated rod in natural sea water, *Int. J. Heat Mass Transf* 95 (2016) 206–213.
- [7] H. Kim, G. DeWitt, T. McKrell, J. Buongiorno, L. Hu, On the quenching of steel and zircaloy spheres in water-based nanofluids with alumina, silica and diamond nanoparticles, *Int. J. Mult. Flow* 35 (2009) 427–438.
- [8] H. Kim, J. Buongiorno, L.-W. Hu, T. McKrell, Nanoparticle deposition effects on the minimum heat flux point and quench front speed during quenching in water-based alumina nanofluids, *Int. J. Heat Mass Transf* 53 (2010) 1542–1553.
- [9] D. Ciloglu, A. Bolukbasi, The quenching behavior of aqueous nanofluids around rods with high temperature, *Nucl. Eng. Des* 241 (2011) 2519–2527.
- [10] S.-Y. Chun, I.C. Bang, Y.-J. Choo, C.-H. Song, Heat transfer characteristics of Si and SiC nanofluids during a rapid quenching and nanoparticles deposition effects, *Int. J. Heat Mass Transf* 54 (2011) 1217–1223.
- [11] G.P. Narayan, K. Anoop, S.K. Das, Mechanism of enhancement/deterioration of boiling heat transfer using stable nanoparticle suspensions over vertical tubes, *J. Appl. Phys* 102 (2007) 074317.
- [12] H. Lotfi, M. Shafii, Boiling heat transfer on a high temperature silver sphere in nanofluid, *Int. J. Therm. Sci* 48 (2009) 2215–2220.
- [13] T.P. Kumar, Influence of steel grade on surface cooling rates and heat flux during quenching, *J. Mater. Eng. Perform* 22 (2013) 1848–1854.
- [14] H. Hasan, M. Peet, J. Jalil, H. Bhadeshia, Heat transfer coefficients during quenching of steels, *Heat Mass Transf* 47 (2011) 315–321.
- [15] S.W. Lee, S.M. Kim, S.D. Park, I.C. Bang, Study on the cooling performance of sea salt solution during reflow heat transfer in a long vertical tube, *Int. J. Heat Mass Transf* 60 (2013) 105–113.
- [16] S.-H. Hsu, Y.-H. Ho, M.-X. Ho, J.-C. Wang, C. Pan, On the formation of vapor film during quenching in de-ionized water and elimination of film boiling during quenching in natural sea water, *Int. J. Heat Mass Transf* 86 (2015) 65–71.
- [17] K. Babu, T.P. Kumar, Mathematical modeling of surface heat flux during quenching, *Metall. Mater. Trans. B* 41 (2010) 214–224.
- [18] S.U. Choi, Nanofluids: from vision to reality through research, 2009 033106.
- [19] K. Babu, T.P. Kumar, Effect of CNT concentration and agitation on surface heat flux during quenching in CNT nanofluids, *Int. J. Heat Mass Transf* 54 (2011) 106–117.
- [20] K. Babu, T.P. Kumar, Estimation and analysis of surface heat flux during quenching in CNT nanofluids, *J. Heat Transfer* 133 (2011) 071501.
- [21] G. Paul, P.K. Das, I. Manna, Rewetting of vertical pipes by bottom flooding using nanofluid as a coolant, *J. Heat Transfer* 137 (2015) 121009.
- [22] K. Rana, G. Agrawal, J. Mathur, U. Puli, Measurement of void fraction in flow boiling of ZnO-water nanofluids using image processing technique, *Nucl. Eng. Des* 270 (2014) 217–226.
- [23] S. Zhou, R. Ni, Measurement of the specific heat capacity of water-based Al⁺ 2O⁻ 3 nanofluid, *Appl. Phys. Lett* 92 (2008) 093123.
- [24] S. Sahu, P. Das, S. Bhattacharyya, An experimental investigation on the quenching of a hot vertical heater by water injection at high flow rate, *Nucl. Eng. Des* 240 (2010) 1558–1568.
- [25] J.P. Holman, *Experimental methods for engineers*, 1966.
- [26] G. Paul, P.K. Das, I. Manna, Assessment of the process of boiling heat transfer during rewetting of a vertical tube bottom flooded by alumina nanofluid, *Int. J. Heat Mass Transf* 94 (2016) 390–402.
- [27] S.W. Lee, S.-Y. Chun, C.H. Song, I.C. Bang, Effects of Al₂O₃ and carbon nanofluids on reflow heat transfer in a long vertical tube.